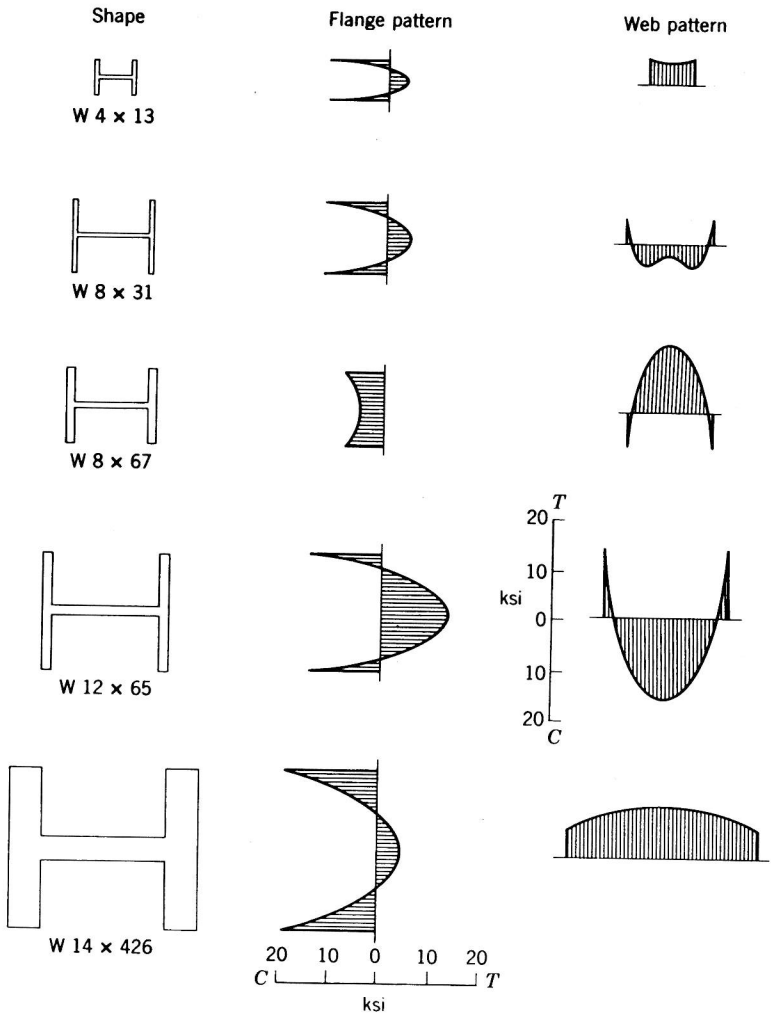

Fig. 3.3 Residual-stress distribution in rolled wide-flange shapes.

The effect of steel grade on the residual-stress distribution is not as great as the effect of geometry (Tall, 1964). Residual-stress measurements in the flanges of similar shapes made of different steel grades show that the distributions and magnitudes of the residual stress are similar and it is here—in the flanges—that residual stresses have a major effect on the column strength of H-shaped sections.

Calculated critical-load column curves based on the residual stresses found in the five particular shapes of Fig. 3.3 are plotted in Fig. 3.5 for buckling about the minor axis, along with maximum strength column curves determined

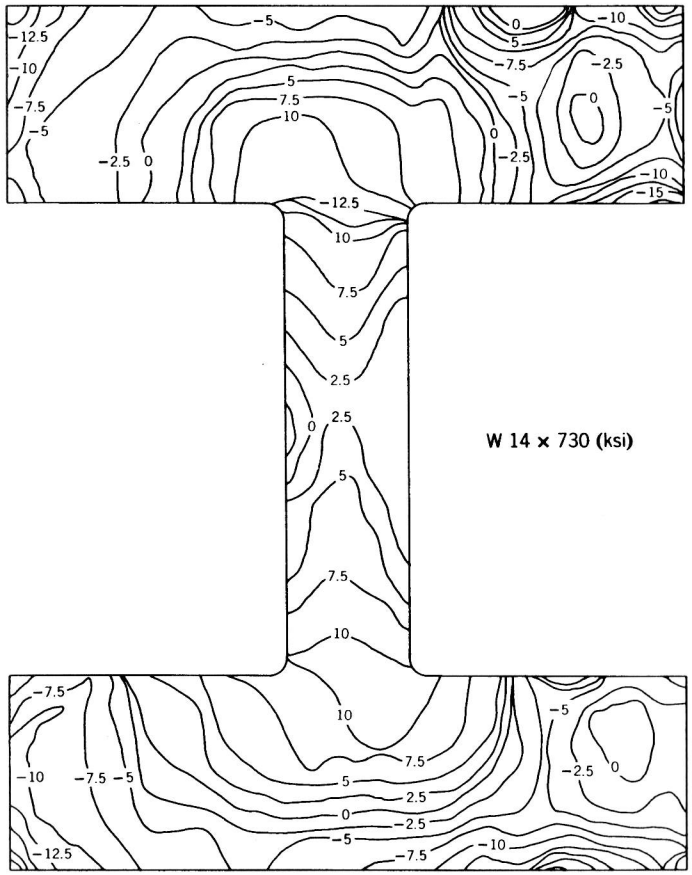

Fig. 3.4 Residual-stress distribution in W14 × 730 shape.

by computer analyses and based on a combination of the measured residual stresses and an initial curvature equal to the maximum tolerated by the ASTM A6 standard.

To interrelate the residual stress and initial curvature effects systematically, extensive column strength analyses were made at the University of Michigan (Batterman and Johnston, 1967). The studies included yield stresses of 36, 60, and 100 ksi (248, 414, and 689 MPa); maximum compressive residual stresses of 0, 10, and 20 ksi (0, 69, and 138 MPa); five curvatures corresponding to initial midlength out-of-straightness ranging from 0 to $0.004L$; and slenderness ratios ranging from 20 to 240. Emphasis was on buckling about the minor axis, and the results of this condition are presented graphically in the work by Batterman and Johnston (1967), permitting maximum-strength evaluation within the range of the parameters cited. On the basis of a maximum residual stress of

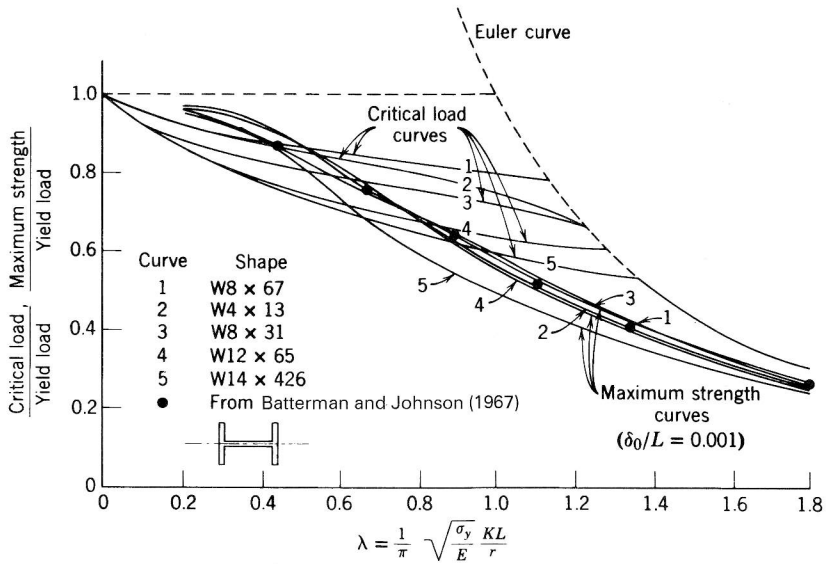

Fig. 3.5 Critical-load curves for straight columns compared with maximum-strength curves for initially curved rolled steel W-shapes.

13 ksi (90 MPa), which is the scaled average maximum for the five sections shown in Fig. 3.3, together with a yield stress of 36 ksi (248 MPa), the maximum column strength predicted by Batterman and Johnston is shown by the solid circles on Fig. 3.5. The solid curves are from an analysis neglecting the webs. Although the shapes and residual stress distributions are different, there is good correlation between the two independently developed analysis procedures. These findings are also corroborated by those of a wide-ranging investigation of column strength (Bjorhovde, 1972), which examined the behavior and strength of a large and diverse number of structural shapes. The computational procedure is very accurate but requires knowledge of the residual stresses and the out-of-straightness. In the study performed at Lehigh University (Bjorhovde, 1972), the full range of structural steel grades and shapes was examined, as well as a number of welded build-up box and H-shapes.

The results obtained by the studies of Batterman and Johnston (1967) and Bjorhovde (1972) show clearly that:

1. The separate effects of residual stress and initial curvature cannot be added to give a good approximation of the combined effect on the maximum column strength. Thus in some cases and for some slenderness ratios, the combined effect is less than the sum of the parts (intermediate slenderness ratios, low residual stresses). In other cases the combined effect is more than the sum of the parts. The latter applies to the intermediate slenderness ratio

range for heavy hot-rolled shapes in all steel grades and for welded built-up H-shapes. It is emphasized that the magnitudes of the maximum compressive residual stresses in a large number of these shapes were 50% or more of the yield stress of the steel itself.

2. Residual stress has little effect on the maximum strength of very slender columns, either straight or initially crooked, which have strengths approaching the Euler load. However, such columns made of the higher-strength steels can tolerate much greater lateral deflection before yield or before becoming unstable.

3. Strengths are slightly underestimated in a computer analysis when based on the assumption that an initial crookedness in the shape of a half-sine wave remains a half-sine wave during further loading.

4. Differences in column strength caused by variations in the shape of the residual stress pattern are smaller for initially crooked columns than for initially straight columns.

More recent data on the residual stresses of very heavy hot-rolled shapes confirmed the findings of Brozzetti et al. (1970a) and demonstrated further that the relative maximum column strength (i.e., computed maximum strength divided by the yield load) reaches a minimum for flange thicknesses around 3 to 4 in (75 to 100 mm). The relative strength increases as the flange thickness exceeds this magnitude (Bjorhovde, 1988; 1991).

Welded Built-Up Columns. Residual stresses resulting either from welding or from the manufacture of the component plates have a significant influence on the strength of welded H- or box-section columns. The maximum tensile residual stress at a weld or in a narrow zone adjacent to a flame-cut edge is equal to or greater than the yield stress of the plates (Alpsten and Tall, 1970; McFalls and Tall, 1970; Alpsten, 1972a; Brozzetti et al., 1970b; Bjorhovde et al., 1972). Welding modifies the prior residual stresses due either to flame cutting or cooling.

Figure 3.6 shows that the strengths of welded columns made of higher-strength steels appear to be influenced relatively less by residual stresses than are the strengths of similar columns made of lower-strength steels (Kishima et al., 1969; Bjorhovde, 1972). It is also evident that the differences in strengths of columns with the maximum permissible initial crookedness are less than the differences in critical loads of initially straight columns (see Fig. 3.5).

As shown in Fig. 3.7, plates with mill-rolled edges (universal mill plates) have compressive residual stresses at the plate edges, whereas flame-cut plates have tensile residual stresses at the edges. In built-up H-shapes made of universal mill plates, the welding will increase the compressive stress at the flange tips, enlarging the region of compressive residual stress and adversely affecting the column strength. Thus, as illustrated in Fig. 3.8, an H-shape column made from flame-cut plates will have favorable tensile residual stresses at the flange

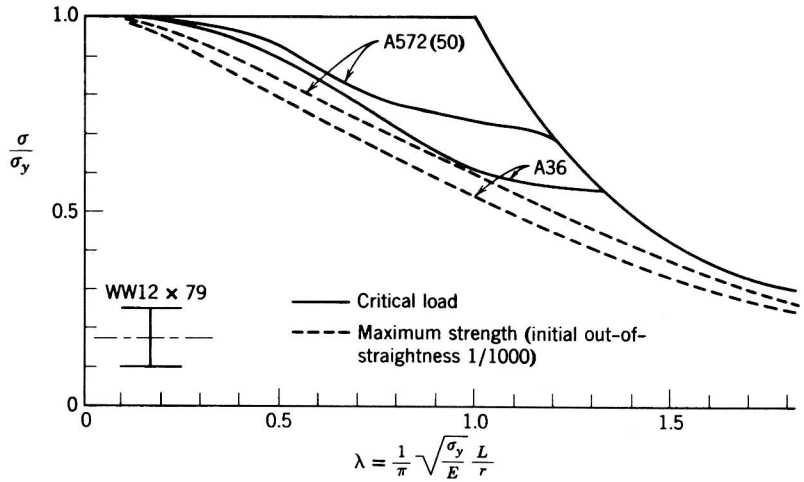

Fig. 3.6 Critical-load curves for welded WW12 × 79 of flame-cut plates compared with maximum-strength curves for initially curved members (Kishima et al., 1969; Bjorhovde, 1972).

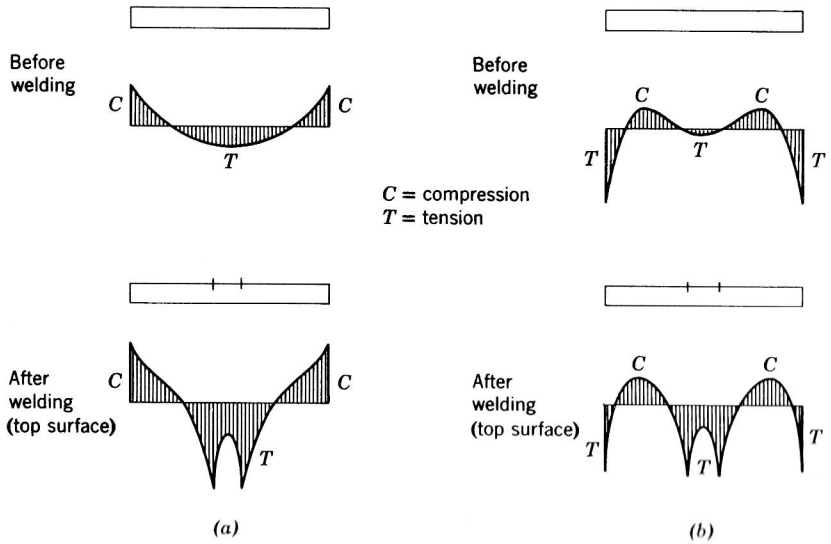

Fig. 3.7 Qualitative comparison of residual stresses in as-received and center-welded universal mill and oxygen-cut plates: (*a*) universal mill plate: (*b*) oxygen-cut plate.

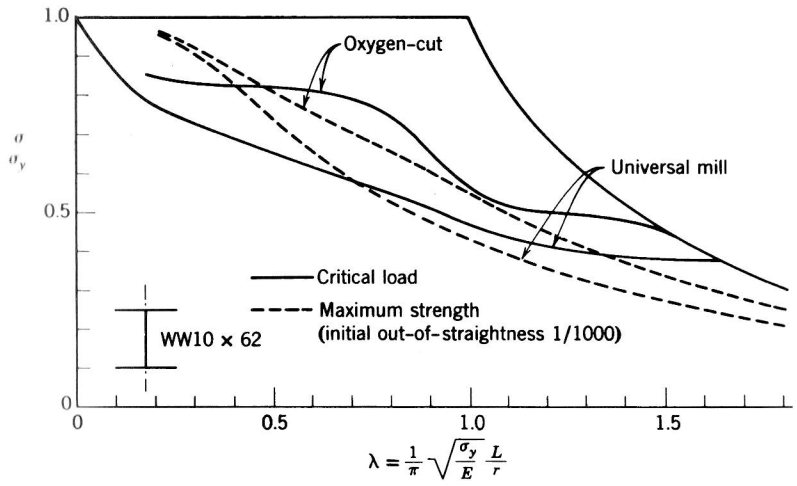

Fig. 3.8 Comparison of column curves for WW10 × 62 (A7 steel) with universal mill versus oxygen-cut plates (Bjorhovde, 1972).

tips. It therefore exhibits greater column strength than that of a column of the same section with flanges consisting of a universal mill plate in which both rolled edges are retained. It is also seen that for short welded columns, the maximum strength of an initially curved column may in some cases be greater than the critical load of a straight column. Obviously, the maximum strength of an initially straight column will always be greater than the critical load of the same column.

Strength differences between box section columns made of universal mill and flame-cut plates are relatively small, because the edge welds override the residual stresses in the component plates (Bjorhovde and Tall, 1971). The sequence of welding can be a significant factor for such columns, particularly for those with large welds (Beer and Tall, 1970).

Several investigations have considered the effects of column size. It has been shown (Kishima et al., 1969; Alpsten and Tall, 1970; Brozzetti et al., 1970b; Bjorhovde et al., 1972), that welding has a greater influence on the overall distribution of residual stress in small and medium-sized shapes than in the case of heavy shapes.

The distribution of residual stress in heavy plates and shapes is not uniform through the thickness (Brozzetti et al., 1970a; Alpsten and Tall, 1970). As thickness increases, the difference between surface and interior residual stresses may be as much as 10 ksi (69 MPa). As an example, Fig. 3.9 shows an isostress diagram for a heavy welded shape made from flame-cut plates. However, it has been found that calculated critical loads and maximum column strengths are only a few percent less when based on the complete residual-stress distribu-

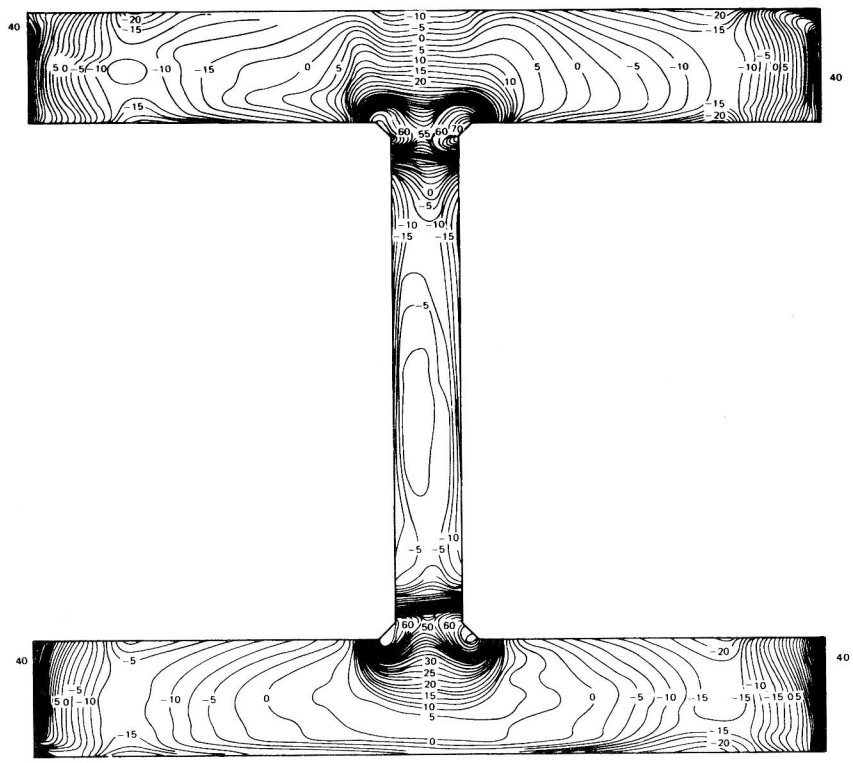

Fig. 3.9 Isostress diagram for WW23 × 681 welded built-up shape (stresses in kips per square inch) (Alpsten and Tall, 1970).

tions, as compared with analyses that assume the stress to be constant through the thickness and equal to the surface-measured residual stress.

In general, shapes made from flame-cut plates exhibit higher strength than shapes that are made from universal mill plates. This is demonstrated by the curves in Fig. 3.10. Similarly, flame-cut shapes tend to have strengths that are comparable with those of similar rolled shapes, whereas universal mill shapes tend to be comparatively weaker (Fig. 3.10).

Figure 3.11 compares the strengths of two typical welded columns with flame-cut flange plates, and one being distinctly heavier than the other. It is seen that the heavier shape tends to be relatively stronger than the lighter one. This is even more accentuated for shapes that are welded from universal mill plates; for these the strength of the lighter shape will be significantly lower than the heavy one (Bjorhovde and Tall, 1971; Bjorhovde, 1972). This is the reason the Canadian Standards Association in its limit-states design standard has since 1974 required that welded built-up shapes can only be made from flame-cut plates. In a major study, Chernenko and Kennedy (1991) examined

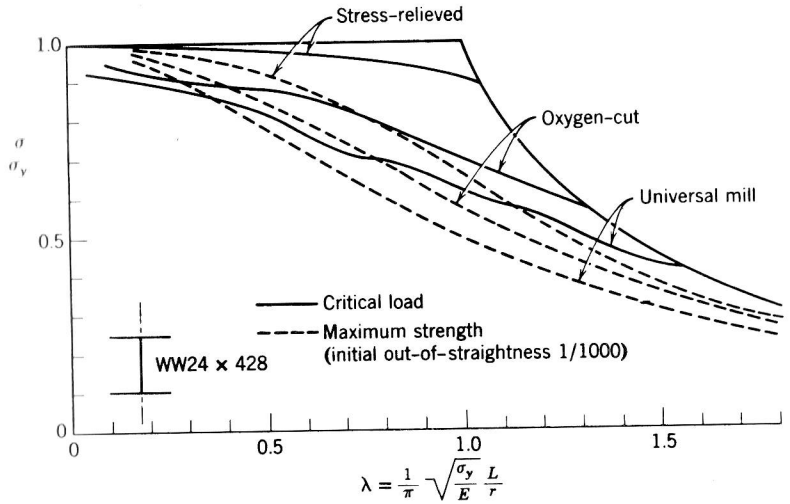

Fig. 3.10 Column curves for heavy and light welded wide-flange shapes (Bjorhovde, 1972).

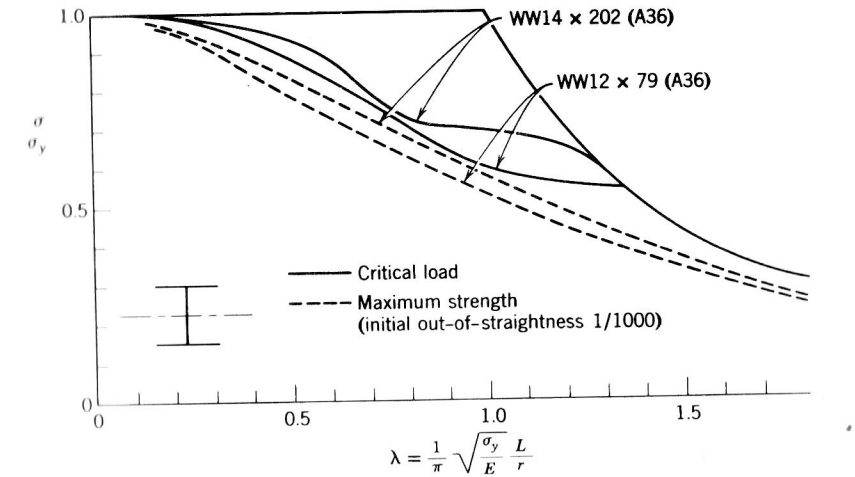

Fig. 3.11 Comparison of column curves for WW24 × 428 (A36 steel) with stress-relieved, oxygen-cut, and universal mill plates (Bjorhovde, 1972).

an extensive range of welded built-up wide-flange shapes. In addition to performing maximum-strength computations for columns with a variety of residual-stress distributions and out-of-straightnesses, the work also examined statistical data on material and other properties. Resistance factors for use with LRFD criteria for welded columns were developed. It is shown that

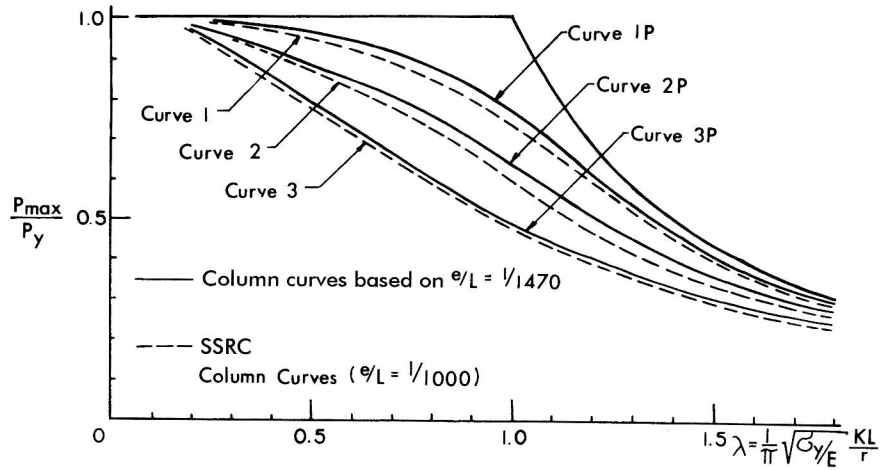

Fig. 3.14 Comparison of multiple column curves developed on the basis of mean out-of-straightness ($L/1470$) and maximum permissible out-of-straightness ($L/1000$) (Bjorhovde, 1972).

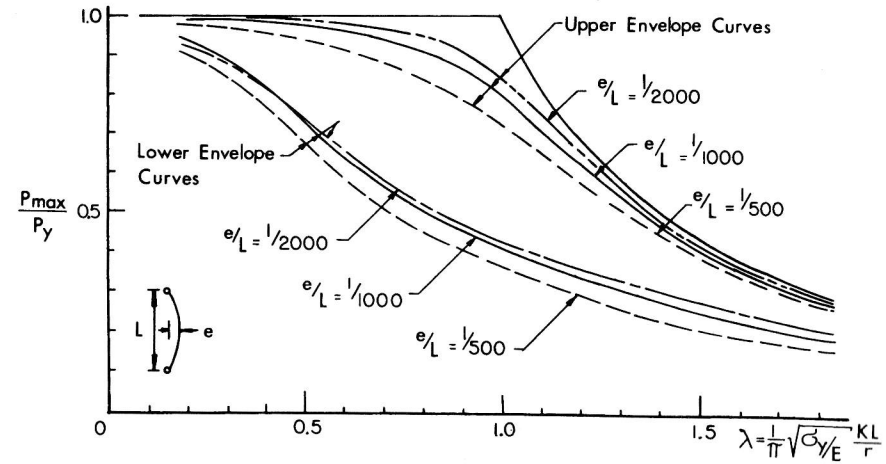

Fig. 3.15 Column curve bands for 112 columns, based on initial out-of-straightnesses of $L/500$, $L/1000$, and $L/2000$ (Bjorhovde, 1972).

1983, 1984), and Shen and Lu (1983), among others. In addition, the analysis of frames with semirigid connections has been dealt with in several studies (DeFalco and Marino, 1966; Romstad and Subramanian, 1970; Frye and Morris, 1975; Ackroyd, 1979; Lui and Chen, 1988; Nethercot and Chen, 1988; Goto et al, 1993; King and Chen, 1993, 1994; Kishi et al., 1993a and b. The column investigations have examined different aspects of restrained member behavior: specifically, determining the influence of:

1. Type of beam-to-column connection
2. Length of column
3. Magnitude and distribution of residual stress
4. Initial out-of-straightness

The frame analysis studies have focused on evaluations of the drift characteristics of frames with less than fully rigid connections, in part prompted by a study by Disque (1975). However, frame-related subjects of this kind are beyond the scope of this chapter. In fact, connection flexibility and member instability are closely related, and their interaction effects can have a significant influence on the overall performance of the frame.

As would be intuitively expected, the stiffness of the restraining connection is a major factor. One illustration of the influence is given by the M–ϕ curves in Fig. 3.16, another by the load-deflection curves for columns with different end restraint that are shown in Fig. 3.17 (Jones et al., 1982). A British wide-flange shape was used for the data generated for Fig. 3.17 incorporating an initial out-of-straightness of $L/1000$. The curves that are shown apply for a slenderness ratio of 120 ($\lambda = 1.31$), but similar data were developed for longer as well as shorter columns. Other investigators have provided additional load-deflection curves, the primary differences between the individual studies are found in the methods of column analysis and end-restraint modeling, but the resulting curves are very similar (Jones et al., 1980, 1982; Razzaq and Chang, 1981); (Sugimoto and Chen, 1982).

Figure 3.17 also includes the load-deflection curve for a pin-ended column. As is evident, the greater the connection restraint, the stiffer will be the initial response of the column, and the greater the maximum load that can be carried as compared to a pin-ended column. The same relative picture emerges for all slenderness ratios, although the magnitude of the increase becomes small for values of l/r 50 and less.

A further illustration of the influence of end restraint is given by the data in Fig. 3.18, which shows column strength curves for members with a variety of end conditions (Jones et al., 1982; Lui and Chen, 1983a). The effect of the connection type is again evident, as is the fact that the influence diminishes for shorter columns. Also included in the figure is the Euler curve, as well as SSRC curve 2 (Bjorhovde, 1972).

It is emphasized that the connections that were used to develop the column curves in Fig. 3.18 are all of the "simple" type. The potential for the structural economies that may be gained by incorporating the end restraint into the column design procedure is clear, although the realistic ranges for the values of λ must be borne in mind and the possible use of bracing to reduce frame drift in designing semirigid frames with flexible base joints must be considered. The ranges for λ have been delineated in Fig. 3.18 for steels with yield stresses of 36 and 50 ksi (248 and 345 MPa). Consequently, the very large column strength increases that have been reported by several researchers are real

A computerized maximum strength analysis was performed first on basic data available from carefully constructed column tests performed at Lehigh University, and it was demonstrated that the method of numerical analysis gave an accurate prediction of the test strengths. Next, a set of 112 column curves was generated for members for which measured residual-stress distributions were available, assuming that the initial crookedness was of a sinuosoidal shape having a maximum amplitude of 1/1000 of the column length and that the end restraint was zero. These shapes encompassed the major shapes used for columns, including rolled and welded shapes from light to heavy dimensions. The column curves thus obtained represent essentially the whole spectrum of steel column behavior. The resulting curves are shown in Fig. 3.22.

Bjorhovde then observed that there were definite groupings among the curves, and from these three subgroups were identified, each giving a single "average" curve for the subgroup (Bjorhovde and Tall, 1971; Bjorhovde, 1972). The resulting three curves are known as *SSRC column strength curves 1, 2, and 3*, and they are reproduced in Figs. 3.23 through 3.25. These figures contain:

1. The number of column curves used as a basis for the statistical analysis and the width of their scatter band
2. The calculated $2\frac{1}{2}$ and $97\frac{1}{2}$ percentile lower and upper probability limits for the particular set of curves
3. The column types to which each of the three curves is related

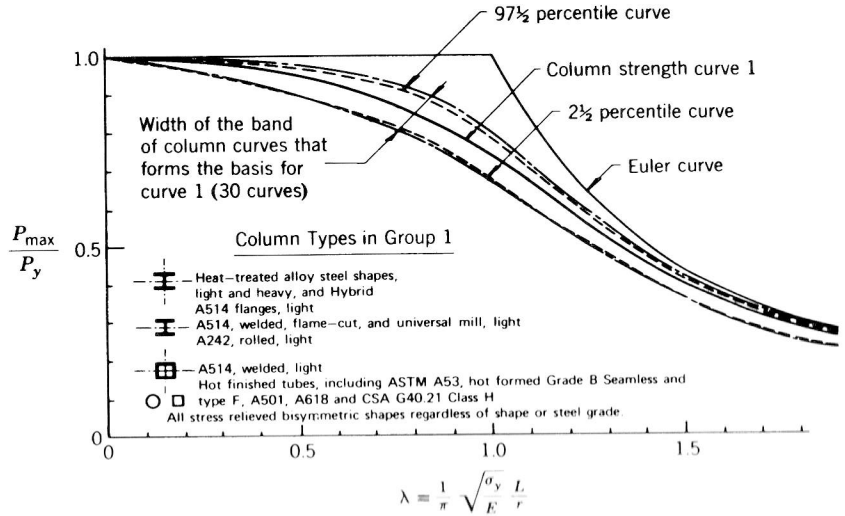

Fig. 3.23 SSRC column strength curve 1 for structural steel (Bjorhovde, 1972). (Based on maximum strength and initial out-of-straightness of $\delta_0 = 0.001L$.)

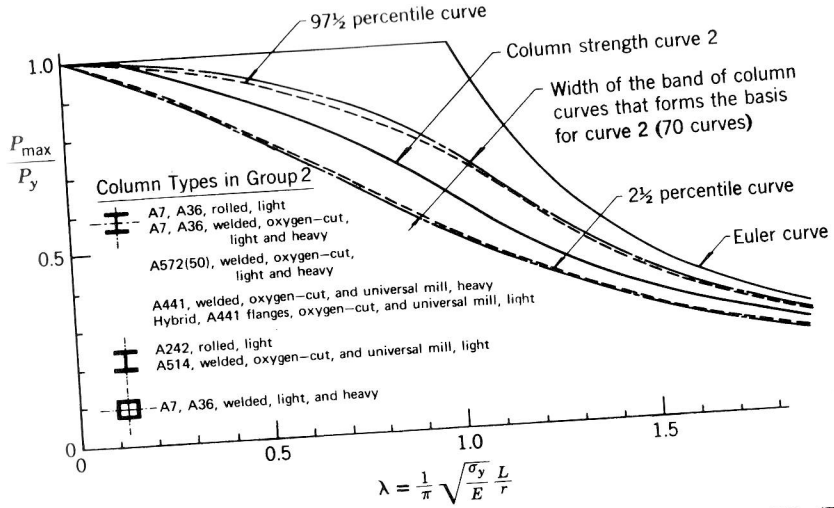

Fig. 3.24 SSRC column strength curve 2 for structural steel (Bjorhovde, 1972). (Based on maximum strength and initial out-of-straightness of $\delta_0 = 0.001L$.)

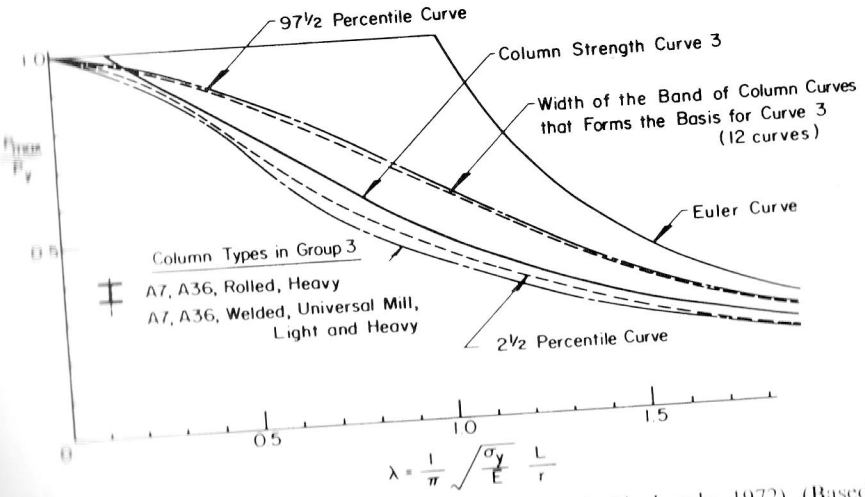

Fig. 3.25 Column strength curve 3 for structural steel (Bjorhovde, 1972). (Based on maximum strength and initial out-of-straightness of $\delta_0 = 0.001L$.)

Algebraic representations of the three column strength curves were obtained by curve fitting, and the resulting equations are as follows;

SSRC curve 1:

$$\left.\begin{array}{lll} 1. & \text{For } 0 \le \lambda \le 0.15 & \sigma_u = \sigma_y \\ 2. & \text{For } 0.15 \le \lambda \le 1.2 & \sigma_u = \sigma_y(0.990 + 0.122\lambda - 0.367\lambda^2) \\ 3. & \text{For } 1.2 \le \lambda \le 1.8 & \sigma_u = \sigma_y(0.051 + 0.801\lambda^{-2}) \\ 4. & \text{For } 1.8 \le \lambda \le 2.8 & \sigma_u = \sigma_y(0.008 + 0.942\lambda^{-2}) \\ 5. & \text{For } \lambda \ge 2.8 & \sigma_u = \sigma_y\lambda^{-2} \ (=\text{Euler curve}) \end{array}\right\} \quad (3.10)$$

SSRC curve 2:

$$\left.\begin{array}{lll} 1. & \text{For } 0 \le \lambda \le 0.15 & \sigma_u = \sigma_y \\ 2. & \text{For } 0.15 \le \lambda \le 1.0 & \sigma_u = \sigma_y(1.035 - 0.202\lambda - 0.222\lambda^2) \\ 3. & \text{For } 1.0 \le \lambda \le 2.0 & \sigma_u = \sigma_y(-0.111 + 0.636\lambda^{-1} + 0.087\lambda^{-2}) \\ 4. & \text{For } 2.0 \le \lambda \le 3.6 & \sigma_u = \sigma_y(0.009 + 0.877\lambda^{-2}) \\ 5. & \text{For } \lambda \ge 3.6 & \sigma_u = \sigma_y\lambda^{-2} \ (=\text{Euler curve}) \end{array}\right\} \quad (3.11)$$

SSRC curve 3:

$$\left.\begin{array}{lll} 1. & \text{For } 0 \le \lambda \le 0.15 & \sigma_u = \sigma_y \\ 2. & \text{For } 0.15 \le \lambda \le 0.8 & \sigma_u = \sigma_y(1.093 - 0.622\lambda) \\ 3. & \text{For } 0.8 \le \lambda \le 2.2 & \sigma_u = \sigma_y(-0.128 + 0.707\lambda^{-1} - 0.102\lambda^{-2}) \\ 4. & \text{For } 2.2 \le \lambda \le 5.0 & \sigma_u = \sigma_y(0.008 + 0.792\lambda^{-2}) \\ 5. & \text{For } \lambda \ge 5.0 & \sigma_u = \sigma_y\lambda^{-2} \ (=\text{Euler curve}) \end{array}\right\} \quad (3.12)$$

These expressions can also be represented quite accurately (maximum deviations −2.1 to +3.6%) by one equation (Rondal and Maquoi, 1979; Lui and Chen, 1984):

$$\sigma_u = \frac{\sigma_y}{2\lambda^2}(Q - \sqrt{Q^2 - 4\lambda^2}) \le \sigma_y \quad (3.13)$$

where

$$Q = 1 + \alpha(\lambda - 0.15) + \lambda^2 \quad (3.14)$$

and

$$\alpha = \begin{cases} 0.103 & \text{for curve 1} \\ 0.293 & \text{for curve 2} \\ 0.622 & \text{for curve 3} \end{cases}$$

Another expression using a single parameter n in a double exponential representation, as used in CSA Standard S16.1-94 (CSA, 1994; Loov, 1995), is

$$\sigma_u = F_y(1 + \lambda^{2n})^{\frac{-1}{n}} \quad (3.15)$$

where $n = 2.24$ for curve 1, 1.34 for curve 2, and 1.00 for curve 3 (the latter is not utilized in the CSA standard). These expressions give strengths generally within 1% of the polynomials of Eqs. 3.10 through 3.12, and are never more than 3% different.

Bjorhovde (1972) also developed multiple column curves where the initial out-of-straightness was equal to its mean value of 1/1470 of the column length (Fig. 3.14). The mathematical equations describing these curves are as follows:

SSRC curve 1P:

$$\left.\begin{array}{lll} 1. & \text{For } 0 \le \lambda \le 0.15 & \sigma_u = \sigma_y \\ 2. & \text{For } 0.15 \le \lambda \le 1.2 & \sigma_u = \sigma_y(0.979 + 0.205\lambda - 0.423\lambda^2) \\ 3. & \text{For } 1.2 \le \lambda \le 1.8 & \sigma_u = \sigma_y(0.03 + 0.842\lambda^{-2}) \\ 4. & \text{For } 1.8 \le \lambda \le 2.6 & \sigma_u = \sigma_y(0.018 + 0.881\lambda^{-2}) \\ 5. & \text{For } \lambda \ge 2.6 & \sigma_u = \sigma_y\lambda^{-2} \ (=\text{Euler curve}) \end{array}\right\} \quad (3.16)$$

SSRC curve 2P:

$$\left.\begin{array}{lll} 1. & \text{For } 0 \le \lambda \le 0.15 & \sigma_u = \sigma_y \\ 2. & \text{For } 0.15 \le \lambda \le 1.0 & \sigma_u = \sigma_y(1.03 - 0.158\lambda - 0.206\lambda^2) \\ 3. & \text{For } 1.0 \le \lambda \le 1.8 & \sigma_u = \sigma_y(-0.193 + 0.803\lambda^{-1} + 0.056\lambda^{-2}) \\ 4. & \text{For } 1.8 \le \lambda \le 3.2 & \sigma_u = \sigma_y(0.018 + 0.815\lambda^{-2}) \\ 5. & \text{For } \lambda \ge 3.2 & \sigma_u = \sigma_y\lambda^{-2} \end{array}\right\} \quad (3.17)$$

SSRC curve 3P:

$$\left.\begin{array}{lll} 1. & \text{For } 0 \le \lambda \le 0.15 & \sigma_y = \sigma_y \\ 2. & \text{For } 0.15 \le \lambda \le 0.8 & \sigma_u = \sigma_y(1.091 - 0.608\lambda) \\ 3. & \text{For } 0.8 \le \lambda \le 2.0 & \sigma_u = \sigma_y(0.021 + 0.385\lambda^{-1} + 0.066\lambda^{-2}) \\ 4. & \text{For } 2.0 \le \lambda \le 4.5 & \sigma_u = \sigma_y(0.005 + 0.9\lambda^{-2}) \\ 5. & \text{For } \lambda \ge 4.5 & \sigma_u = \sigma_y\lambda^{-2} \ (=\text{Euler curve}) \end{array}\right\} \quad (3.18)$$

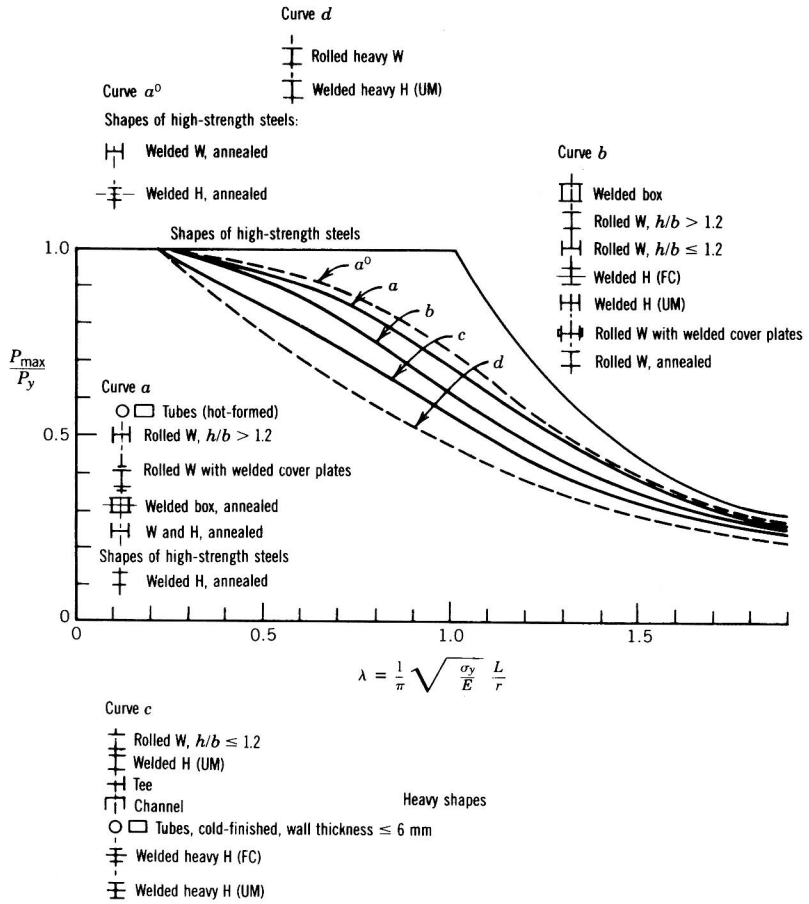

Fig. 3.26 European multiple column curves, recommended by the European Convention for Constructional Steelwork (ECCS 1978). (Based on initial out-of-straightness, $\delta_0 = 0.001L$.)

tabulated for use with effective-length-factor alignment charts, or should the design curves implicitly contain minimal end restraints? The latter approach was used in the development of the AISC–LRFD column curve, which is based on an implicit end restraint producing an elastic effective-length factor of 0.96 ($G = 10$), as well as an initial out-of-straightness of 1/1500 of the length.

Summary. In the previous discussion on the strength of steel columns a number of alternatives were presented. Specification writing groups need to make decisions to select the column curve satisfying their needs and wishes. The necessary theory is available to do so, and much information is on hand. It is the SSRC's firm opinion that design criteria for steel columns should be based on the initially crooked column with residual stresses. With

Column Curve Selection Table

Fabrication Details		Axis	Specified Minimum Yield Stress of Steel (ksi) ≤ 36	37 to 49	50 to 59	60 to 89	≥ 90
Hot rolled W shapes	Light and medium W-shapes	Major	2	2	1	1	1
		Minor	2	2	2	1	1
	Heavy W-shapes (flange over 2 in.)	Major	3	2	2	2	2
		Minor	3	3	2	2	2
Welded Built up H shapes	Flame-cut plates	Major	2	2	2	1	1
		Minor	2	2	2	2	1
	Universal mill plates	Major	3	3	2	2	2
		Minor	3	3	3	2	2
Welded Box Shapes	Flame-cut and universal mill plates	Major	2	2	2	1	1
		Minor	2	2	2	1	1
Square and Rectangular tubes	Cold-formed	Major	N/A	2	2	2	2
		Minor	N/A	2	2	2	2
	Hot-formed and cold-formed heat-treated	Major	1	1	1	1	1
		Minor	1	1	1	1	1
Circular tubes	Cold-formed	N/A	2	2	2	2	2
	Hot-formed	N/A	1	1	1	1	1
All stress relieved Shapes		Major and Minor	1	1	1	1	1

Fig. 3.27 Column curve selection table (Bjorhovde, 1972, 1988).

this concept as a basis, intelligent choices for column design can be made, resulting in a rational method of design.

3.8.7 Aluminum columns

Material Properties. Alloying elements, heat treatment, and working have a great influence on all the essential properties of aluminum, with the exception of the elastic modulus, which falls within the range 9900 to 10,200 ksi (68 to 70 GPa) for other than aircraft alloys. In general engineering, a value of 10,000 ksi (68.3 GPa) is used.

Yield strength is more strongly influenced by heat treatment and working than is the ultimate strength. For heat-treated or strain-hardened alloys there is also an increased sharpness of the "knee" between the elastic and plastic ranges, which is significant for columns in the lower range of slenderness ratios. For this reason column formulas for aluminum alloys are divided into two groups, heat-treated and non-heat-treated, which reflect the differing ratio $\sigma_{0.2}/\sigma_{0.1}$. Alloys that are solution heat-treated but not artificially aged, seldom used in engineering, fall in the non-heat-treated group. Guaranteed values for the yield strength, defined by the 0.2% offset, and the ultimate strength are established at levels at which 99% of the material is expected to conform at a